BEAM LOSS SIMULATIONS FOR THE IMPLEMENTATION OF THE HARD X-RAY SELF-SEEDING SYSTEM AT EUROPEAN XFEL

S. Liu†, W. Decking, L. Fröhlich, DESY, Hamburg, Germany

Abstract

The European XFEL is designed to be operated with a nominal beam energy of 17.5 GeV at a maximum repetition rate of 27000 bunches/second. The high repetition rate together with the high loss sensitivity of the undulators raises serious radiation damage concern, especially for the implementation of the Hard X-ray Self-Seeding (HXRSS) system, where a 100 μm thick diamond crystal will be inserted close to the beam in the undulator section. Since the seeding power level highly depends on the delay of the electron beam with respect to the photon beam, it is crucial to define the minimum electron beam offset to the edge of the crystal in the HXRSS chicane. At European XFEL a ~200 m long post-linac collimation section has been designed to protect the undulators. In the HXRSS scheme, however, beam halo particles hitting the crystal can generate additional radiation. Particle tracking simulations have been performed using GEANT4 and BDSIM for the undulator and the collimation section, respectively. The critical number of electrons allowed to hit the crystal is estimated for a certain operation mode and the efficiency of beam halo collimation is investigated to predict the minimum HXRSS chicane delay.

INTRODUCTION

The Hard X-ray Self-Seeding (HXRSS) is a well-known scheme to increase the X-ray longitudinal coherence [1]. At European XFEL [2], the HXRSS will be first equipped at the SASE2 (3-25 keV) photon beam line. In order to reduce the heat load on the 100 μm thick diamond crystal a 2 cascades system will be implemented (see Fig. 1). This scheme can also significantly increase the signal to noise ratio of the photon spectrum, thus generating Fourier transform-limited X-ray pulses [3].

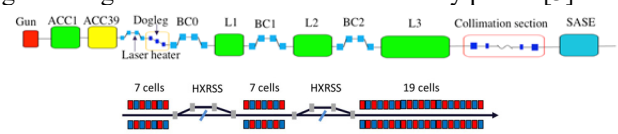

Figure 1: Schematic layout of European XFEL beam line (top) and HXRSS in SASE2 (bottom).

One of the most important parameters, which determine the performance of HXRSS, is the seeding power level. The seeding power level highly depends on the delay of the electron beam with respect to the photon beam (i.e. the horizontal offset of the e- beam in the chicane). With a delay increase of 10 fs (~0.5 mm increase of offset), the seeding power can decrease by a factor 2 [4]. Since the crystal is inserted to "filter" the frequency of the photon beam, the electron beam offset also refers to the distance of the electron beam center to the crystal edge, which is critical for the radiation protection (beam halo particles hitting the crystal can generate additional radiation). At LCLS and SACLA, where the HXRSS has already been implemented, the minimum distances from the crystal edge to the beam are set to be ~2.5 mm, which permits a seeding with ~20 fs delay [5,6]. For European XFEL, however, due to the much higher repetition rate[1], there is more concern about radiation damage. Therefore, it is crucial to study the crystal insertion position limit.

At European XFEL, a ~200 m long post-linac collimation section has been designed to protect the undulators. This section is designed as a second order achromatic and first-order isochronous section to satisfy the requirement of an energy acceptance of ±1.5% of the nominal energy. Particle tracking simulations through the collimation section had been performed during its design [7]. The simulation results showed that the R=3 mm aperture in the collimation section is enough to protect an undulator vacuum chamber with 3 mm radius. However, in these simulations, secondary particles generation and scattering were not included, and the collimators were considered as "black absorber" (i.e. any particle touching them is considered as lost). In the HXRSS scheme, however, beam halo particles, which lost only a small fraction (<1.5%) of their energy in the collimation section (e.g. by scattering), may still be transported to the undulator section and hit the crystal.

Therefore, for the HXRSS implementation, we first performed GEANT4 [8] simulation with simplified geometry in the undulator section to estimate the critical number of beam halo particles allowed to hit the crystal. And then we used BDSIM[2] [9] to track a uniformly distributed beam halo particle distribution through the collimation section to study the maximum number of beam halo particles that are able to reach the crystal.

ESTIMATION OF CRITICAL NUMBER OF BEAM HALO PARTICLES

High energy electrons hitting the diamond crystal can generate high energy photons which can in turn generate photonuclear process in different materials downstream of the HXRSS system. Fast neutrons generated in photonuclear processes are considered to be the main source of demagnetization of permanent Nd-Fe-B magnets [10]. GEANT4 simulations have been performed to estimate the maximum neutron fluence generated by the 17.5 GeV e- beam hitting the 100 μm diamond crystal.

† shan.liu@desy.de

[1] The maximum repetition rate is 4.5 MHz at European XFEL, 120 Hz at LCLS and 60 Hz at SACLA.

[2] BDSIM is a toolkit of GEANT4 and it extends the ability of GEANT4 to allow for fast geometry building and fast tracking with design optics.

ISBN 978-3-95450-182-3

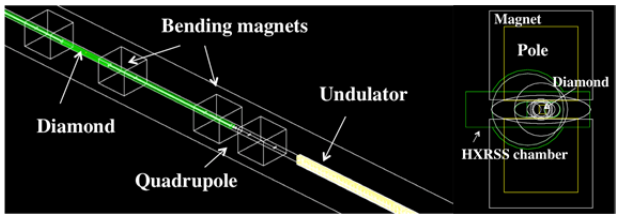

Figure 2: GEANT4 geometry layout (left) and apertures of different components (right).

A simplified geometry is applied in GEANT4, as shown in Fig. 2, with the aperture of each component shown on the right plot. Quadrupoles, chicane magnets, absorbers, undulator magnet and poles, vacuum chambers and the diamond crystal are included in the geometry with the same longitudinal dimensions as in the design of the HXRSS and undulator sections. The quadrupoles and bending magnets are approximated as iron boxes with a cylindrical hole in the center.

Physics list QGSP_BERT_HP is used in the simulation. This list includes a high precision neutron package that can transport the neutrons below 20 MeV down to thermal energies. A biasing factor of 50 is applied to the Bremsstrahlung production inside the diamond crystal and to the photonuclear cross section in all the materials[3].

The simulation starts at the 1st HXRSS section (which is located in the 8th undulator section) followed by 7 undulators plus a 2nd HXRSS section and another 19 undulators (see Fig. 1). For the first simulation, 10^7 electrons are generated, which hit the crystal with normal incidence. The simulation results are shown in Fig. 3.

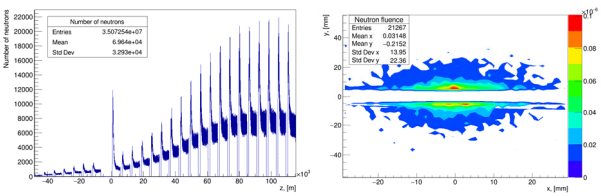

Figure 3: Number of neutrons along the undulators starting from the first HXRSS section (left) and transverse distribution of the neutron fluence at the location with maximum number of neutrons (right).

The left plot in Fig. 3 shows the histogram of the number of neutrons ($N_{neutrons}$) along the beam line. Note that the 0 position is set to the beginning of the undulator section right after the 2nd HXRSS section, where a large jump of $N_{neutrons}$ can be observed. Similar spikes can be found at the beginning of each undulator section, since at this location the undulator magnets and poles are exposed directly to the radiation shower generated by the quadrupoles in the inter-sections between two undulators. The following magnets and poles are, however, more and more protected by the "self-shielding". Thus, we observe a decrease of $N_{neutrons}$ after the spikes. $N_{neutrons}$ reaches maximum at around 134 m (~22nd undulator sections) downstream of the 1st HXRSS section. This value is quite close to the estimated typical distance of bremsstrahlung impact (L) based on the characteristic angle (θ_e) of emission for thin-target bremsstrahlung: $L = R/\tan\theta_e = \frac{R}{\tan\left(\frac{m_e}{E_e}\right)} \approx 137$ m, where $R = 25$ mm is the radius of the vacuum chamber, and E_e is the electron beam energy [10].

Figure 3 right plot shows the transverse distribution of the neutron fluence at the location with maximum $N_{neutrons}$ along the undulator beam line (beginning of the 22nd undulator). It can be seen that the maximum neutron fluence is located in the center of the magnet with the value of ~10^{-7} n/cm^2/e$^-$. The maximum neutron flux allowed for 0.01 % demagnetization[4] of Nd-Fe-B magnets is measured experimentally in Ref. [11] to be ~1×10^{11} n/cm^2. Therefore, if we assume 0.01% demagnetization of the magnets in 20 years with 10 shifts (8 hours each) /month for HXRSS operation (i.e. 6.912×10^7 seconds), the maximum allowed number of e$^-$/bunch (with 27000 bunches/s) can be calculated as:

$$N_{critical} = \frac{10^{11}}{6.912\times10^7\times27000\times10^{-7}} \approx 5\times10^5\ \mathrm{e^-/bunch}. \quad (1)$$

Comparing with the maximum charge per bunch: N_{total} =1nC ≈ 6.25×10^9 e-/bunch, the maximum allowed number of e-/bunch is around 10^{-4} of N_{total}[5]. This number will be further compared with the maximum number of beam halo particles that may hit the crystal estimated in the following section.

TRACKING SIMULATION IN COLLIMATION SECTION

Tracking simulations with ±50 sigma beam halo particles uniformly distributed in the (x,xp,y,yp) 4D phase space [13] have been performed in BDSIM[3]. The beam halo particles distribution is matched to the design optics at the beginning of the collimation section and tracked through the section using BDSIM. Four main collimators made of titanium with inner radius of 2 mm and three supplementary collimators made of aluminium with inner radius of 10 mm are used in the simulation[6].

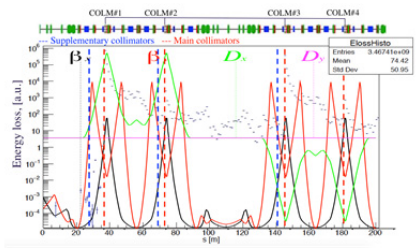

Figure 4: Energy loss map and the design optics (not to scale) along the collimation section.

[3] In GEANT4 the production cuts for the e$^-$, e$^+$ and γ are set as 0.1 μm in the crystal, 1 μm in the undulator region and 0.7 mm in the other regions. In BDSIM cut of 0.7 mm is used for all particles in all regions.

[4] This is the maximum allowed demagnetization to preserve FEL performance without retuning the undulators [11].

[5] This is a rough estimation, since no transverse position or angular distributions of the e$^-$ are taken into account and the electrons are considered as monochromatic. Besides, note that GEANT4 can underestimate the photon neutron production by ~30% according to Ref. [12].

[6] The main collimators can be moved vertically to change the apertures (2 mm, 3 mm, 4 mm and 10 mm are available), while the apertures of the supplementary collimators are fixed as 10 mm. For tracking convenience, the horizontal and vertical coordinates are exchanged.

The energy loss map along the collimation section with the design optics and the locations of the collimators are shown in Fig. 4. Since the collimation section is designed as a "dogleg", the secondary photons and neutrons can not reach the undulator section. On the other hand, the electrons that lost only a small fraction of their energy (e.g. due to scattering on the collimator or chamber wall) can still be transported up to the undulator section.

Figure 5 (a) and (b) shows the histogram of energy distribution of the primary and secondary electrons at the end of the four main collimators with 10^5 input electrons. One can see that at COLM#1 and COLM#3 more low energy secondary electrons are produced than at COLM#2 and COLM#4. This is due to the fact that COLM#1 and COLM#3 are the first main collimators in the first and second arcs (see Fig. 4), and the phase space is rotated by 90° between them, so most primary betatron and angular halo particles are collimated by them. In the end of COLM#4 there are only few secondary electrons with less than 2 GeV energy left. We assume that those secondary electrons would get lost in the bending magnet after the COLM#4 and only those primary electrons, which lost a small fraction of their energy (<1.5%), can reach the undulators. In order to increase the statistics of these electrons, we repeated the simulation with 10^7 input electrons without recording the secondary particles.

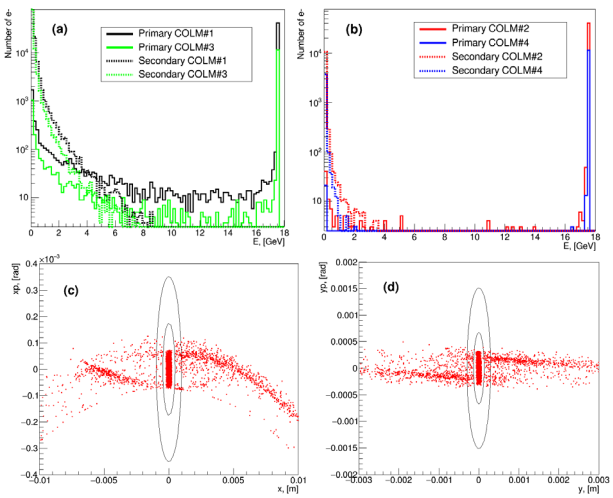

Figure 5: Energy distribution of the primary and secondary beam halo particles at the end of COLM#1 and COLM#3 (a) and at end of COLM#2 and COLM#4 (b) with 10^5 input electrons; Phase space distributions at the end of the collimation section for the horizontal (c) and vertical (d) plane with 10^7 input electrons.

Figure 5 (c) and (d) shows the phase space distribution at the end of the collimation section for the primary particles with energy higher than 17.2375 GeV with 10^7 input electrons. The dynamic aperture in the undulator section with radius R=4 mm (minimum undulator aperture) and R=2 mm are also shown in Fig. 5 as two ellipses. Particles outside the dynamic aperture of the undulator chamber will be stopped at the undulator entrance and only the particles inside the aperture may reach the crystal location, which is 7 undulators downstream. The center part are the particles which can pass through the collimator freely, and the particles between the R=2 mm and R=4 mm apertures are those which may hit the crystal (assuming that the crystal is 2 mm away from the beam center).

By estimating the number of electrons between the two ellipses (N_{hits}) and comparing this number with the maximum allowed number of electrons ($N_{critical}$) calculated in Eq. (1), one can set the minimum distance that the crystal can approach to the beam center (i.e. the minimum HXRSS chicane delay). In the case that the crystal is 2 mm away from the center, N_{hits} is estimated to be 27±6 out of the total number of electrons $N_{total}=10^6$. This is 3 times lower than $N_{critical}$, which is estimated as 10^{-4} of N_{total}. Note that in our simulation the input transverse beam distribution is uniform, while the normal beam should be Gaussian-like, which can reduce N_{hits} dramatically. Meanwhile, the crystal will be inserted horizontally from the side of the beam, which means only half of the horizontal halo particles can hit the crystal. Therefore, with the conditions mentioned before, and assuming that there is no additional beam halo particles generation after collimation section, we can conclude that the crystal can be inserted to a minimum distance of 2 mm from the beam center, which means a chicane delay of ~13 fs.

CONCLUSIONS AND PROSPECTS

We have performed beam halo particles tracking simulations for the implementation of HXRSS at European XFEL. Using a simplified geometry in GEANT4 we first studied the maximum number of beam halo particles allowed to hit the diamond crystal ($N_{critical}$). Then, in order to estimate the number of beam halo particles that may hit the crystal (N_{hit}), we tracked a uniformly distributed beam halo particles through the collimation section (with 2 mm apertures) using BDSIM. Finally, by extracting the number of electrons which can pass through the aperture of the undulators and can hit the crystal inserted to 2 mm from the beam center, we conclude that, even in this worst scenario, N_{hit} is ~3 times smaller than $N_{critical}$. Therefore, we can safely insert the crystal down to 2 mm from the beam center (i.e. a minimum chicane delay of ~13 fs) with the 2 mm collimator apertures.

Further simulations can be performed with more realistic beam halo particles distribution and with different collimator apertures. Similar beam loss studies can also be carried out for other applications with very tight aperture requirement (e.g. corrugated structure [14], afterburner undulator). It is also possible to include the GEANT4 model with undulators in BDSIM and perform a start to end beam halo particles tracking.

ACKNOWLEDGEMENTS

The authors would like to thank colleagues at DESY and European XFEL: I. Agapov, V. Balandin, G. Feng, G. Geloni, N. Golubeva, J. Pflueger and many colleagues from LCLS, especially J. Welch, H.-D. Nuhn and M. Santana-Leitner, for helpful discussions. And thanks to S. Boogert and L. Nevay from RHUL for their support on BDSIM.

ISBN 978-3-95450-182-3

REFERENCES

[1] G. Geloni, V. Kocharyan and E. Saldin, "A novel self-seeding scheme for hard X-ray FELs", *Journal of Modern Optics*, 58(16), pp.1391-1403, 2011.

[2] M. Altarelli, R. Brinkmann *et al.*, "XFEL: The European X-Ray Free-Electron Laser Technical Design Report", DESY, Hamburg, Germany, DESY 2006-097, 2006.

[3] G. Geloni, V. Kocharyan and E. Saldin, "A Cascade self-seeding scheme with wake monochromator for narrow-bandwidth X-ray FELs", DESY, Hamburg, Germany, DESY 10-080, June 2010.

[4] S. Liu and W. Decking, "Self-Seeding implementation at European XFEL", 8th Hard X-ray FEL Collaboration Meeting, Pohang, South Korea, Oct. 2016.

[5] J. Amann *et al.*, "Demonstration of self-seeding in a hard-X-ray free-electron laser", *Nature photonics*, 6 (10), pp. 693-698, 2012.

[6] T. Inagaki *et al.*, "Hard x-ray self-seeding set-up and results at SACLA", in *Proc. FEL' 14*, Basel, Switzerland, Aug. 2014, paper TUC01, pp. 603-608.

[7] V. Balandin, R. Brinkmann, W. Decking, and N. Golubeva, "Optics Solution for the XFEL Post-Linac Collimation Section", DESY, Hamburg, Germany, TESLA-FEL Report 2007-05, 2007.

[8] S. Agostinelli *et al.*, "GEANT4—a simulation toolkit", *Nucl. Instr. Meth. A*, vol. 506(3), pp. 250-303, 2003.

[9] I. Agapov *et al.* "BDSIM: A particle tracking code for accelerator beam-line simulations including particle–matter interactions" *Nucl. Instr. Meth. A*, vol. 606(3), pp. 708-712, 2009.

[10] A. Fasso, "Dose Absorbed in LCLS Undulator Magnets, I. Effect of a 100 μm Diamond Profile Monitor", SLAC, Menlo Park, USA, Radiation Physics Note, RP-05-05, May 2005.

[11] M. Santana-Leitner *et al.*, "Radiation protection studies for LCLS tune up dump", SLAC, Menlo Park, USA, SLAC-PUB-14020. 2010.

[12] L. Quintieri *et al.*, "Comparison of validations of GEANT4 and FLUKA codes on photo-nuclear predictions in the high-energy range", 13th Meeting on Shielding Aspects of Accelerators, Targets and Irradiation Facilities (SATIF-13), Dresden, Germany, Oct. 2016.

[13] R. Yang *et al.*, "Modeling and Experimental Studies of Beam Halo at ATF2", in *Proc. 7th Int. Particle Accelerator Conf. (IPAC'16)*, Busan, South Korea, May 2016, paper MOPMB008, pp. 88-91.

[14] I. Zagorodnov, G. Feng and T. Limberg, "Corrugated structure insertion for extending the SASE bandwidth up to 3% at the European XFEL", *Nucl. Instr. Meth. A*, vol. 837, pp. 69-79, 2016.